bioRxiv preprint doi: https://doi.org/10.1101/2020.01.10.901991; this version posted January 11, 2020. The copyright holder for this preprint (which was not certified by peer review) is the author/funder, who has granted bioRxiv a license to display the preprint in perpetuity. It is made available under aCC-BY-NC-ND 4.0 International license.

Talin Folding; the Tuning Fork of Cellular Mechanotransduction

Rafael Tapia-Rojo[1,*] and Julio M. Fernandez[1]

[1] *Department of Biological Sciences, Columbia University, New York, NY 10027, USA*

Cells continually sample their mechanical environment using exquisite force sensors such as talin, whose folding status triggers mechanotransduction pathways by recruiting binding partners. Mechanical signals in biology change quickly over time and are often embedded in noise; however, the mechanics of force-sensing proteins have only been tested using simple force protocols, such as constant or ramped forces. Here, using our magnetic tape head tweezers design, we measure the folding dynamics of single talin proteins in response to mechanical noise and cyclic force perturbations. Our experiments demonstrate that talin filters out mechanical noise but detects periodic force signals over a finely-tuned frequency range. Hence, talin operates as a mechanical bandpass filter, able to read and interpret frequency-dependent mechanical information through its folding dynamics. We describe our observations in the context of stochastic resonance, which we propose as a mechanism by which mechanosensing proteins could respond accurately to force signals in the naturally noisy biological environment.

* rt2605@columbia.edu

bioRxiv preprint doi: https://doi.org/10.1101/2020.01.10.901991; this version posted January 11, 2020. The copyright holder for this preprint (which was not certified by peer review) is the author/funder, who has granted bioRxiv a license to display the preprint in perpetuity. It is made available under aCC-BY-NC-ND 4.0 International license.

I. INTRODUCTION

The precise interpretation of complex mechanical signals underpins a vast range of biological processes [1–3]. These force signals are accurately detected by cellular force sensors and transduced into electrical or biochemical signals to trigger a physiological response—mechanotransduction [4, 5]. For instance, the human auditory system converts complex vibration patterns into electrophysiological signals with astonishing speed and accuracy, detecting frequencies from 20 to 20,000 Hz with a sensitivity finer than the music interval and a dynamic range greater than 120 dB [6, 7]. Akin to sound waves, mechanical signals in biology oscillate at frequencies that span over several timescales and, yet, are effectively decomposed and interpreted by cells. Additionally, noise is a protagonist at the molecular and cellular level, so every mechanical communication is challenged by a background of non-informative fluctuations that, still, do not interfere with a robust cellular response [8]. However, how molecular force sensors interpret complex mechanical signals in a finely-tuned way remains mostly unknown.

Cells continuously receive and transmit mechanical signals between neighbor cells and the extracellular matrix, which guides diverse processes such as embryonic development [9], cell traction [10], or tumor proliferation [11]. These force stimuli are transduced into biochemical signals, generally by inducing conformational changes in force-bearing proteins that modulate the affinity of binding partners or induce posttranslational modifications [4, 12, 13]. For instance, cells migrate following the stiffness gradient of their substrate, which is sampled by periodic forces applied by focal adhesions—durotaxis [14, 15]. Talin is a mechanosensing hub protein in focal adhesions, which crosslinks transmembrane integrins with the active F-actin filaments and recruits several binding proteins to control the function and fate of this organelle [16–18]. For example, vinculin binds to cryptic helices in mechanically unfolded talin domains, subsequently recruiting actin filaments that reinforce the cellular junction [13, 19–21]. Hence, talin transduces mechanical forces through its folding dynamics.

The mechanics of talin have been studied using force spectroscopy techniques, which typically apply ramped or constant forces to monitor folding or unfolding reactions [22, 23]. These studies have shown that force drives talin response by unfolding each of the 13-rod bundle domains hierarchically; increasing forces result in a gradual unfolding of the talin rod [24, 25]. This response establishes a simple mechanotransduction pathway; the force load on talin determines the number of unfolded talin domains and, hence, how many vinculin molecules can be recruited. However, the response of talin under complex mechanical signals has never been studied, so it remains unknown how talin folding dynamics couple to forces that change in time or if its response is affected when the perturbation is buried in noise.

Here, we measure the folding dynamics of the talin R3 domain under complex force signals, which include mechanical noise and sinusoidal perturbations. Using our new magnetic tape head tweezers design (Fig. 1 A), we demonstrate that talin rejects mechanical noise but exhibits phase-locked folding dynamics when subject to oscillating forces. Talin response is finely tuned, and it only detects signals over a narrow frequency range, which is defined by its mechanical stability; the R3 WT domain responds to signals around 7 Hz, while the more stable R3 IVVI mutant detects slower signals at 1 Hz. We ascribe our results to the physical phenomenon of stochastic resonance, which we propose as a mechanism by which force-sensing proteins could interpret complex mechanical signals through their folding dynamics, by operating as a "biochemical Fourier transform."

II. RESULTS

A. Mechanical Characterization of Talin R3 Domain

The talin R3 domain is the weakest of all 13-rod domains, thought to be the precursor of talin-based adhesions, given its low unfolding force and the presence of two vinculin-binding sites [16, 21, 24, 25]. This low mechanical stability is due to the four-residue threonine belt on its hydrophobic core; the substitution of these residues in the mutant R3 IVVI increases its stability significantly [16, 21]. Due to these different mechanical properties, we explore both the R3 WT and R3 IVVI domains perturbed by complex mechanical signals, which will allow us to compare and relate their responses with their mechanics. First, in order to establish the benchmarks for the study under complex force signals, we characterize the folding mechanics of both domains at constant force (Fig. 1).

Figures 1B and C show representative recordings measured at the coexistence force ($F_{1/2}$; same occupation of the folded and unfolded states), which is 9 pN for R3 IVVI, and 5 pN for R3 WT. Their folding dynamics are characterized by reversible transitions between the folded and unfolded states with an extension change of ∼20 nm, but the kinetics of R3 WT is nearly 10 times faster, compared to those of R3 IVVI (Fig. 1C, inset). From equilibrium trajectories as these, we measure the relative occupation of the folded state (folding probability; Fig. 1D), and the folding (r_F) and unfolding (r_U) rates (Fig. 1E). The folding probability spans less than 2 pN, illustrating the exquisite force sensitivity of both domains. Due to this steep force dependency, the folding and unfolding rates have an exponential

bioRxiv preprint doi: https://doi.org/10.1101/2020.01.10.901991; this version posted January 11, 2020. The copyright holder for this preprint (which was not certified by peer review) is the author/funder, who has granted bioRxiv a license to display the preprint in perpetuity. It is made available under aCC-BY-NC-ND 4.0 International license.

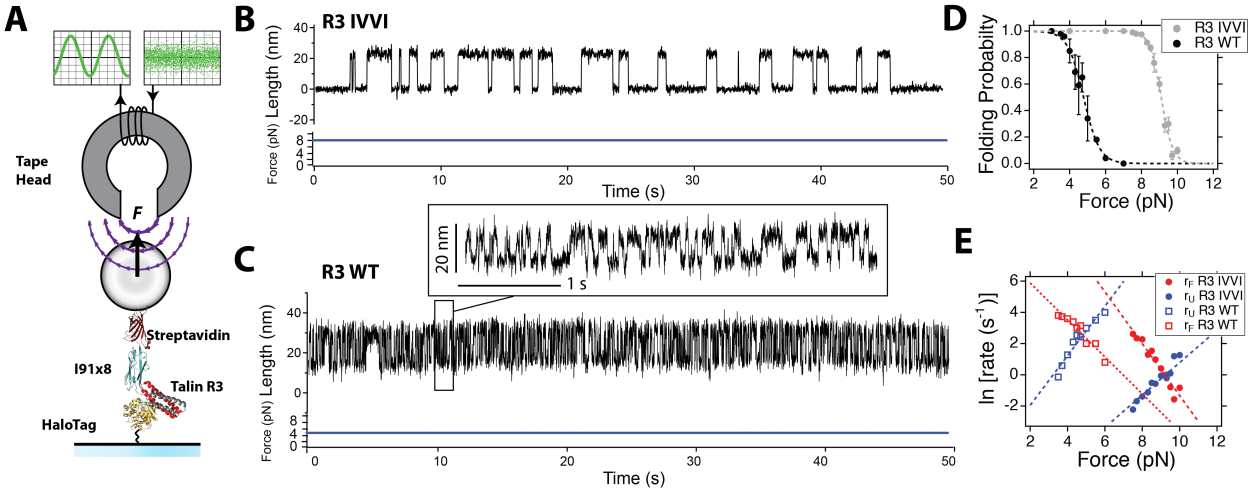

FIG. 1. **Mechanical characterization of talin R3 domain:** (A) Schematics of our magnetic tweezers assay for applying complex force signals to single proteins. Our construct contains talin R3 domain followed by eight repeats of titin I91 domain, flanked by a HaloTag for covalent anchoring to the glass surface and a biotin for interaction with streptavidin-coated magnetic beads. Forces with a bandwidth greater than 10 kHz are generated using a magnetic tape head. (B) Typical single-molecule recording of talin R3 IVVI at 9 pN. (C) Typical recording of talin R3 WT at 5 pN. (Inset) Detail of the trajectory, highlighting the faster dynamics of R3 WT compared to the mutant R3 IVVI. Traces acquired at a frame rate between 1 and 1.5 kHz and smoothed with a Savitzky-Golay 4th-order filter, with a 101-points box (R3 IVVI) and a 31-points box (R3 WT). (D) Folding probability of R3 IVVI and R3 WT talin domains. The R3 IVVI mutant has higher mechanical stability, and its folding probability is shifted to higher forces by 4 pN. (E) Folding (red) and unfolding (blue) rates for R3 IVVI (solid) and R3 WT (empty) talin domains. At the coexistence force, the rates of the WT are $\sim$12 s^{-1}, compared to the slower ones of R3 IVVI ($\sim$1.5 s^{-1}). Data fitted with Bell model (dotted lines), yielding distances to transition states $x_{\mathrm{F}}^{\dagger} = 4.85 \pm 0.56$ nm, and $x_{\mathrm{U}}^{\dagger} = 6.49 \pm 0.66$ nm for R3 WT, and $x_{\mathrm{F}}^{\dagger} = 6.78 \pm 0.59$ nm, $x_{\mathrm{U}}^{\dagger} = 4.27 \pm 0.34$ nm for R3 IVVI.

Bell-like dependency ($\mathrm{r}_{\mathrm{U/F}} = k_0^{\mathrm{U/F}} \exp[\pm F x_{\mathrm{U/F}}^{\dagger}/kT]$ [26]), with similar distances to transition state from the folded and unfolded states. Overall, both domains exhibit two-state like dynamics, occurring at different force ranges—between 4 and 6 pN (R3 WT), and 8 to 10 pN (R3 IVVI)—and kinetic rates on a very different timescale—at $\mathrm{F}_{1/2}$, $\mathrm{r}_{F/U} \approx$12 s^{-1} (R3 WT), and $\mathrm{r}_{F/U} \approx$1.5 s^{-1} (R3 IVVI).

B. Talin Discerns between Mechanical Noise and Oscillatory Forces

Motivated by the naturally noisy cellular environment, we first asked if talin maintains a robust response when subject to a randomly fluctuating perturbation instead of a constant force. Applying forces that change rapidly is challenging, as force spectrometers typically change the force by displacing large mechanical probes. To this aim, we take advantage of our new magnetic tape head tweezers design, able to change the force with a bandwidth higher than 10 kHz while maintaining intrinsic force-clamp conditions (Fig. 1A, [27]). We generate mechanical noise as a broadband uncorrelated force signal, with an average of 9 pN and a peak-to-peak amplitude greater than 7 pN (see Fig. S1 for details) and apply it to the talin R3 IVVI domain. This signal fluctuates around $F_{1/2}$ over a force range that significantly exceeds the folding regime of R3 IVVI.

Figure 2A (left) shows the dynamics of R3 IVVI perturbed by mechanical noise. Strikingly, despite the fine force sensitivity of talin and the broad force range over which the mechanical noise fluctuates, we do not observe any effect on talin dynamics, which are indistinguishable from those measured at the average force of 9 pN. The dwell-time histograms—obtained using a maximum-likelihood procedure (Fig. S2)—are both exponential distributions with approximately the same time constant—0.59 ± 0.02 s (noise) versus 0.69 ± 0.02 s (no noise) (Fig. 2A, right). We observe this behavior at any other folding force, and the folding probability measured in the presence of noise is identical to that measured at constant forces (Fig. S3). This evidence indicates that talin has a robust mechanical response, filtering out randomly fluctuating components, and responding only to the average force.

Given the ability of talin to remain indifferent to noise, we explore its response under a force signal that oscillates at a specific frequency and is submerged in mechanical noise. We build this signal by adding a sinusoidal force $F(t) = F_0 + A\sin(2\pi f_\Omega)$ (with $F_0 = 9$ pN, $A = 1$ pN and $f_\Omega = 0.7$ Hz) to mechanical noise with the same properties employed before. Hence, the amplitude of the correlated component is small compared to the background fluctuations

bioRxiv preprint doi: https://doi.org/10.1101/2020.01.10.901991; this version posted January 11, 2020. The copyright holder for this preprint (which was not certified by peer review) is the author/funder, who has granted bioRxiv a license to display the preprint in perpetuity. It is made available under aCC-BY-NC-ND 4.0 International license.

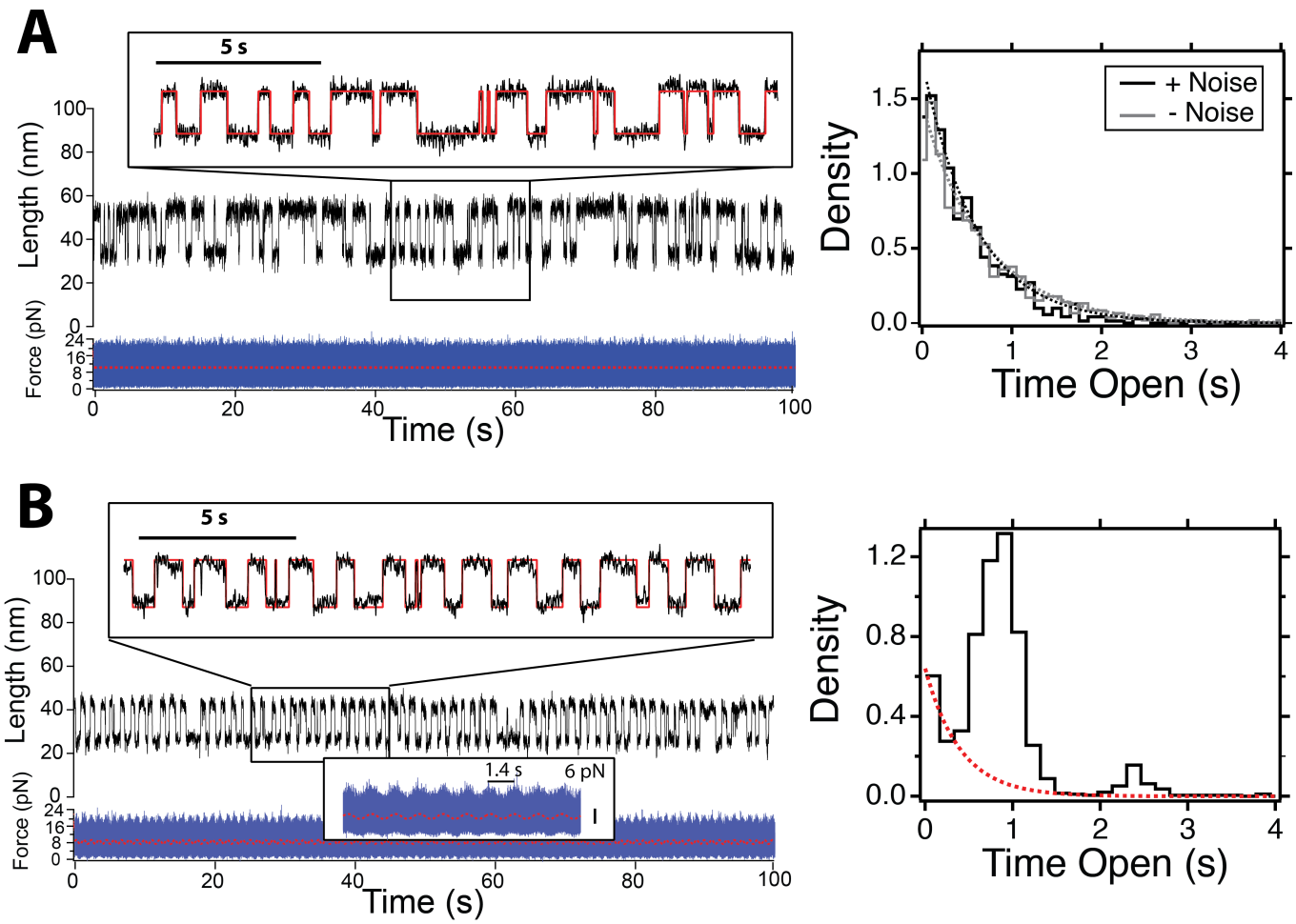

FIG. 2. **Talin detects oscillatory signals among mechanical noise:** (A) (Left) Dynamics of the talin R3 IVVI domain under mechanical white noise with an average of 9 pN and a standard deviation of 2.8 pN. (Inset) Detail of the trajectory, with the idealized trace (red). (Right) Comparison of the dwell-time histograms in the unfolded state perturbed by a constant force of 9 pN (grey) and mechanical noise (black). Both distributions are comparable, as talin remains insensitive to randomly fluctuating forces and responds only to the average perturbation. Histograms built from 1063 (no noise) and 704 transitions (noise). (B) (Left) Dynamics of talin R3 IVVI domain perturbed by a force signal oscillating at 0.7 Hz, with an amplitude of 1 pN, and submerged in white noise with a standard deviation of 2.8 pN. (Right) Dwell-time histogram measured for such a signal. The folding transitions are synchronized with the oscillating force, while the noise is ignored. These dynamics shift the shape of the dwell-time distribution, which shows resonance peaks at odd multiples of half the period of the signal. The remanent stochastic behavior is appreciated as an underlying exponential distribution (red dotted line). Histogram built with 2295 transitions. Traces acquired at a frame rate of 1-1.5 kHz, and smoothed with a Savitzky-Golay 4th order algorithm with a 101-points box size.

(Fig. 2B, force inset). By contrast, talin dynamics are now dramatically altered, and most transitions occur at regular intervals of ∼0.7 s, while the mechanical noise is ignored (Fig. 2B, left). These entrained folding dynamics shift the shape of the dwell-time histogram from an exponential to a peaked distribution (Fig. 2B, right). The first peak is centered at ∼0.7 s, which coincides with half-period of f_Ω, while the second peak appears at three times that value, ∼2.1 s. Despite the dominant entrained dynamics, we observe an underlying exponential distribution, which reflects a minority of remanent stochastic transitions, occurring at a time constant compatible to a force of 9 pN (Fig. 2B, right, red dotted line). Hence, unlike random force fluctuations, talin detects force oscillations through its folding dynamics, which shift from stochastic—characterized by exponentially-distributed dwell-times—, to a phase-locked response, reflected in peaked dwell-time distributions.

bioRxiv preprint doi: https://doi.org/10.1101/2020.01.10.901991; this version posted January 11, 2020. The copyright holder for this preprint (which was not certified by peer review) is the author/funder, who has granted bioRxiv a license to display the preprint in perpetuity. It is made available under aCC-BY-NC-ND 4.0 International license.

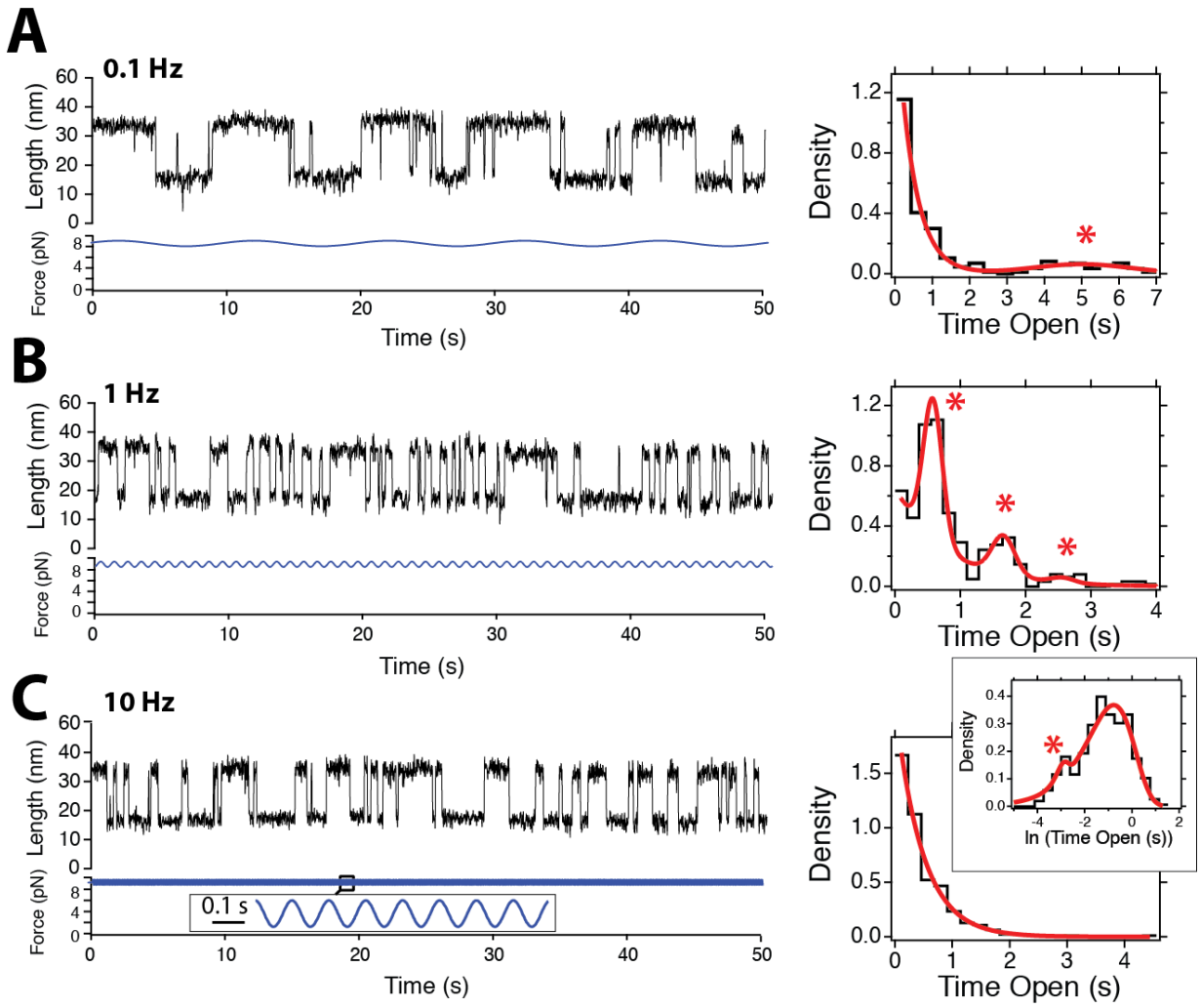

FIG. 3. **Dynamics of talin R3 IVVI domain under signals of different frequencies:** (A, B, C) (Left) 50 seconds-long fragments of magnetic tweezers recordings showing R3 IVVI domain under a periodic signal with an amplitude of 0.7 pN, and frequencies of 0.1, 1, and 10 Hz, respectively. (Right) Dwell time histograms on the unfolded state calculated for each of these signals. The interplay between the stochastic and resonant dynamics is manifested as a combination of exponential and gaussian distributions, with relative weights that indicate the level of response (red fits). At 0.1 Hz, most transitions are stochastic, and only a small peak at 5 s appears (red star). At 1 Hz the response is optimal and the majority of the histogram is built by gaussian peaks, located at odd multiples of half-period of the driving signal (red stars). At a high frequency of 10 Hz, the distribution is exponential, and only a logarithmic binning reveals a small proportion of resonant transitions at 0.05 s (inset, red star). Histograms built with 223 (A), 337 (B) and 363 (C) transitions. Traces acquired at a frame rate between 1 and 1.5 kHz. Traces are smoothed with a Savitzky-Golay 4th-order filter, with a 101-points box.

C. Mechanical Signal Detection by Talin is Frequency-Dependent

The talin R3 domain detects minimal force changes through its folding dynamics; differences in force of only 0.3 pN shift the folding probability by up to 30% (Fig. 1D). Since our data demonstrates that talin detects oscillatory forces, we seek to test if such a response is also frequency-sensitive. To this aim, we subject R3 IVVI to purely oscillating forces at different frequencies, $f_\Omega = 0.1$, 1, and 10 Hz, with a mean value of $F_0 = 9$ pN, and amplitude of $A = 0.7$ pN.

Figure 3 shows R3 IVVI folding dynamics under these three oscillatory force signals (left), with the associated dwell-time histograms (right). Under the slowest perturbation ($f_\Omega = 0.1$ Hz; Fig. 3A), we observe that, while the extension of the protein follows the oscillation, most transitions are stochastic as the force changes much more slowly than the natural folding kinetics—0.1 Hz versus ∼1.5 Hz. The dwell-time histogram is an exponential distribution with a time constant compatible to a constant force of 9 pN ($r_K = 2.16 \pm 0.15$ s^{-1}), and a marginal contribution of entrained transitions as a small peak at 5 s (red star). At $f_\Omega = 1$ Hz (Fig. 2B), most folding transitions are synchronized with the perturbation and occur at regularly spaced time intervals. The dwell-time histogram has three peaks of

bioRxiv preprint doi: https://doi.org/10.1101/2020.01.10.901991; this version posted January 11, 2020. The copyright holder for this preprint (which was not certified by peer review) is the author/funder, who has granted bioRxiv a license to display the preprint in perpetuity. It is made available under aCC-BY-NC-ND 4.0 International license.

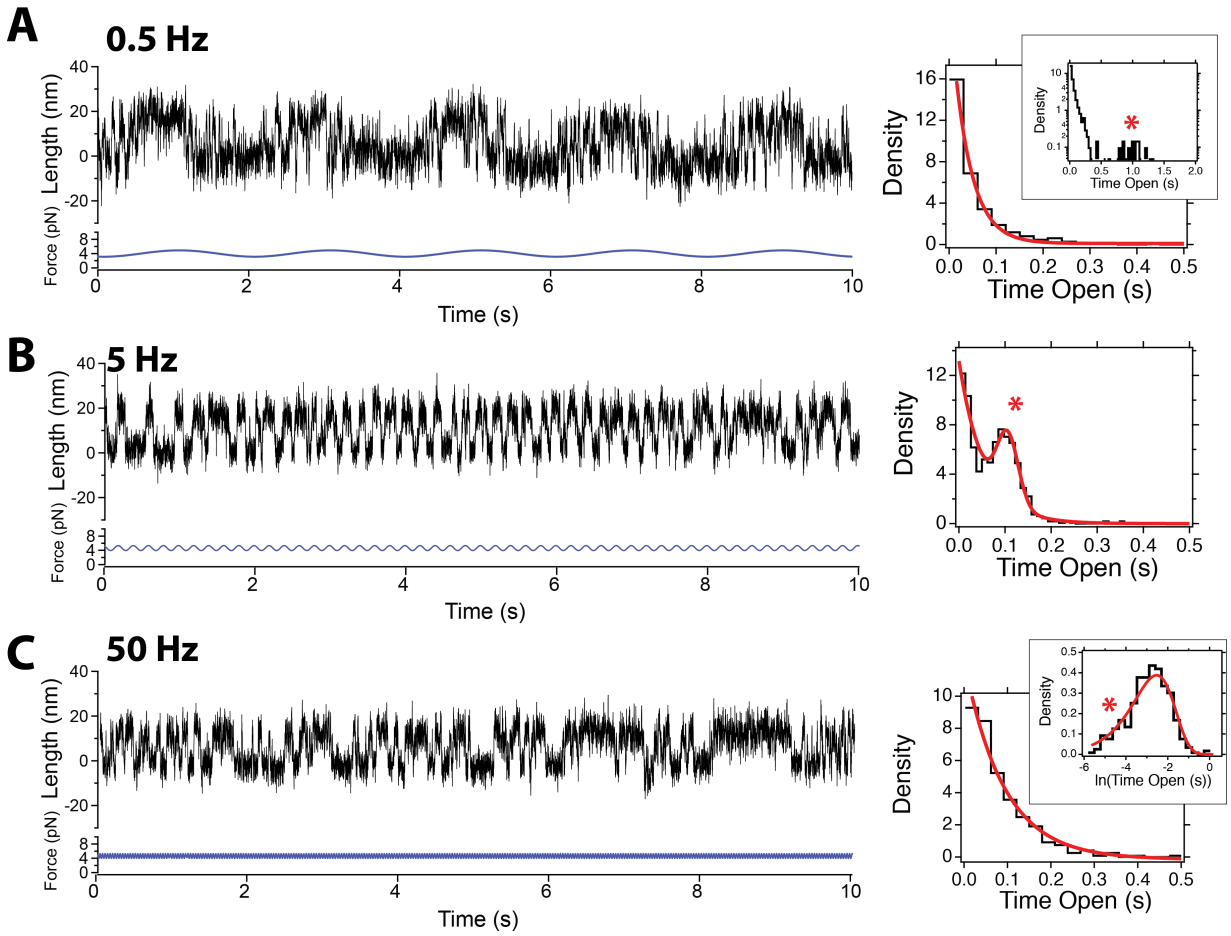

FIG. 4. **Response of R3 WT domain under signals of different frequencies:** (A, B, C) (left) 10 seconds-long fragments of magnetic tweezers recordings showing R3 WT under a sinusoidal force signal with an amplitude of 0.7 pN, and frequencies of 0.5, 5, and 50 Hz, respectively. (Right) Dwell time histograms on the unfolded state, for each of these signals. The WT domain has faster rates than the R3 IVVI, and responds to higher frequencies. Histograms built with 715 (A), 2736 (B), and 1945 (C) transitions. Raw traces are shown, acquired at rates of 1-1.5 kHz.

diminishing amplitude and a small underlying exponential distribution. These peaks are centered at odd multiples of half the driving period—0.5, 1.5, and 2.5 seconds—and represent harmonics on talin phase-locked response. Finally, at a driving frequency of 10 Hz (Fig. 3C), the stochastic behavior is recovered with the same dynamics as those measured at 9 pN. The dwell-time histogram is an exponential distribution with a time constant of $r_K = 2.13 \pm 0.10$ s^{-1}, which indicates that talin filters this fast oscillation. Only when calculating the dwell-time distribution with logarithmic binning, we observe a small contribution at 0.05 s corresponding to a minority of entrained transitions. Hence, these data indicate a frequency-selective response of talin upon oscillating forces. Interestingly, talin folding dynamics segregate into phase-locked dynamics that respond to the oscillation with a frequency-dependent intensity, and a stochastic behavior that filters the signal and detects only the average of the perturbation.

D. Talin Response is Governed by the Mechanical Stability of the Domain

The response of the R3 IVVI domain suggests that the entrained dynamics manifest optimally at frequencies of the order of the natural folding rates, which at 9 pN are $\sim$1.5 s^{-1} (Figure 1E). Hence, it can be expected that proteins with faster kinetic rates will respond to higher frequencies and vice versa, providing a tuning mechanism based on the mechanical stability of the protein domain. In order to test this hypothesis, we measure the folding dynamics of the R3 WT domain subject to oscillatory forces given that, at the coexistence force $F_{1/2} = 5$ pN, its kinetic rates are nearly 10 times faster ($\sim$13 s^{-1}; Fig. 1E).

bioRxiv preprint doi: https://doi.org/10.1101/2020.01.10.901991; this version posted January 11, 2020. The copyright holder for this preprint (which was not certified by peer review) is the author/funder, who has granted bioRxiv a license to display the preprint in perpetuity. It is made available under aCC-BY-NC-ND 4.0 International license.

Figure 4 shows single-molecule recordings of R3 WT perturbed with sinusoidal signals of 0.5 (A), 5 (B), and 50 Hz (C), an average of $F_0 = 5$ pN, and amplitude of $A = 0.7$ pN. These data show an analogous response to that measured for R3 IVVI but shifted to higher frequencies. At 0.5 Hz, the dynamics are exponentially distributed, with a minor entrained contribution appreciable in log-scale (Fig. 4A, inset). At 5 Hz, the transitions are entrained with the force signal, showing a peak at 0.1 s and an underlying exponential distribution with a time constant compatible to that measured at 5 pN ($r_K = 18.0 \pm 2.24$ s^{-1}). At 50 Hz, the dynamics are stochastic with a rate of $r_K = 11.0 \pm 0.8$ s^{-1} and a minimal contribution at 0.01 s appreciable with logarithmic binning (inset). These results suggest the generality of the frequency-dependent signal detection by talin folding dynamics, where the mechanical stability of the protein domain selects the responsive frequency regime. Additionally, we tested R3 WT under mechanical noise and confirmed that it also filters out random fluctuations (Fig. S4).

E. Stochastic Resonance in Talin Folding Dynamics

Our observations show a phase-locked response of talin folding dynamics as a mechanism of mechanical signal detection. This behavior resembles the physical phenomenon of stochastic resonance, by which non-linear systems exhibit an amplified response upon a weak input signal due to the addition of noise [28, 29]. Stochastic resonance has been demonstrated in very diverse contexts, such as climate dynamics [30], optical systems [31], DNA hairpin dynamics [32], or quantum systems [33] since it only requires three fundamental ingredients: an activation barrier, a weak periodic input, and an intrinsic source of noise, all fulfilled by talin under force. Importantly, different from the external mechanical noise we have applied to the system, the noise that amplifies the response refers to the intrinsic stochasticity inherent to the system, which, in our case, is provided by the thermal bath.

Signal detection by stochastic resonance typically refers to an increase in the signal-to-noise ratio of the system output [28]. Indeed, our data shows that, while talin folding dynamics at constant force have a flat power spectrum rate-limited by the system diffusivity, under a periodic forcing, they exhibit a resonance peak at the driving frequency f_Ω (Fig. S5). From our data, we can directly quantify talin response by the shape of the dwell-time distributions, modeled as the sum of an exponential distribution and a Gaussian peak:

$$f(t) = A_\mathrm{s} e^{-r_K t} + A_\mathrm{r} e^{-(t-T_\Omega/2)^2/\sigma}, \tag{1}$$

where r_K is the stochastic folding rate of talin (exponential contribution), $T_\Omega = 1/f_\Omega$ the period of the driving force, and A_s and A_r the amplitudes of the stochastic and resonant contributions, respectively. When the frequency is in the responsive regime, occasionally, several peaks appear at odd multiples of half the driving period ($3(T_\Omega/2)$, $5(T_\Omega/2)$, ...), like those in Fig. 3B. These contributions correspond to higher order harmonics and are included as resonant contributions. Hence, we can quantify statistically the fraction of resonant transitions F_R as the relative weight between the Gaussian distributions and the underlying exponential one. If the distribution is normalized ($\int f(t)dt = 1$), $F_\mathrm{R} = 1 - A_\mathrm{s}/r_K$.

To demonstrate the response of talin over a broad range of frequencies, we carry out experiments on both the R3 IVVI and R3 WT domains under signals with $A = 0.7$ pN and frequencies ranging from 0.05 to 100 Hz. Figure 5A shows F_R as a function of the driving frequency f_Ω. At frequencies above r_K, the resonant peak can be buried in the shape of the exponential distribution, and it is not possible to directly determine its contribution. In such cases, we calculate the dwell-time histogram with logarithmic binning to separate fast timescales and estimate the relative weight from a logarithmic transform of Eq. 1 (Figs. S6 and S7).

Figure 5A shows that talin operates as a mechanical bandpass filter, responding only over a narrow frequency range defined by the mechanical stability of the protein domain. For a bistable system, the optimal resonance frequency can be estimated as $r_K/2$ [28] (red dotted line), which agrees with the experimental data. This resonance frequency is associated with the height of the intrinsic free energy barrier that separates the folded and unfolded states. Oscillating forces tilt the protein landscape towards the folded and unfolded states cyclically, increasing and decreasing the barrier periodically. If this periodic forcing occurs on a timescale compatible with the thermal-activated transitions, the state switching synchronizes with the perturbation. If the driving frequency is much faster than the intrinsic rates, the system responds only to the average barrier, filtering the oscillation; if the oscillation is too slow, the transitions are much more frequent than the timescale imposed by the external forcing.

All these experiments were done with signals of constant amplitude, $A = 0.7$ pN, which is a moderate perturbation compared to the folding probability. In order to test the limit of signal detection, we measure the response of R3 IVVI at the resonance frequency $f_\Omega = 0.7$ Hz and under different amplitudes (Fig. 5B). When the force signal spans the whole folding probability range (A>1 pN), the resonant response is saturated, and nearly all transitions are entrained with the periodic forcing. Under signals as small as 0.3 pN, we still observe an effect of resonant transitions of nearly 15%. This amplitude-dependent response is identical when the signal is buried in mechanical noise (grey squares).

bioRxiv preprint doi: https://doi.org/10.1101/2020.01.10.901991; this version posted January 11, 2020. The copyright holder for this preprint (which was not certified by peer review) is the author/funder, who has granted bioRxiv a license to display the preprint in perpetuity. It is made available under aCC-BY-NC-ND 4.0 International license.

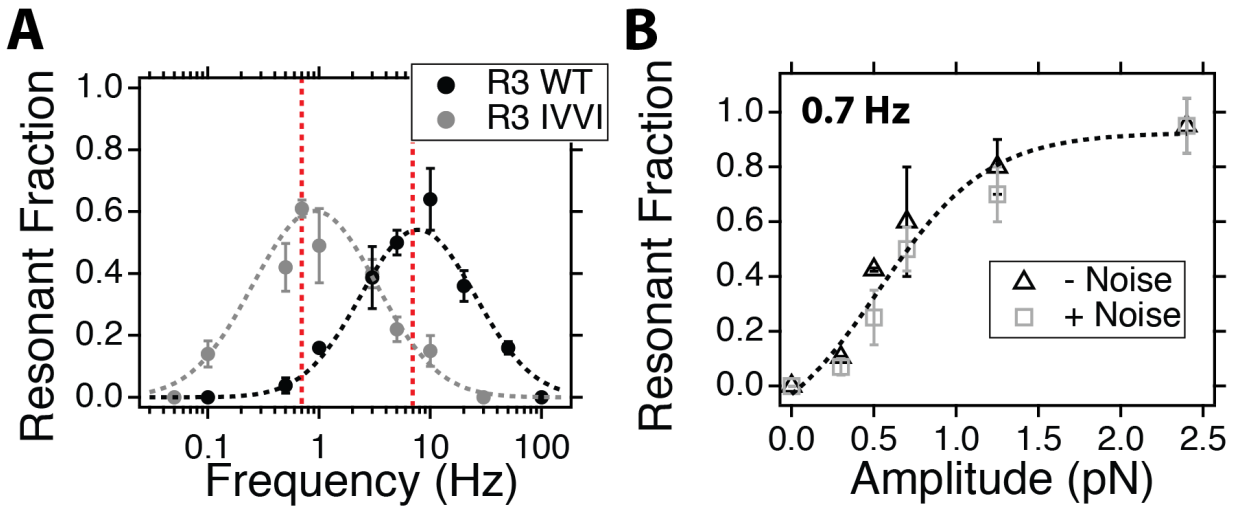

FIG. 5. **Quantitative characterization of stochastic resonant dynamics by talin:** (A) Fraction of resonant transitions for the R3 WT (black) and R3 IVVI (grey) domains. We characterize the level resonant dynamics as the relative weight of the Gaussian-distributed transitions as measured from fits to the dwell-time distributions. Both domains show an optimal frequency range for signal detection around 10 Hz for R3 WT and 1 Hz for R3 IVVI. Higher frequencies are filtered, while lower ones show a majority of stochastic transitions due to the slow oscillation. Red lines show the theoretical resonance frequency, based on the natural folding rates at the coexistence force. The histograms and fits used to determine F_{R} are shown in Figs. S6 and S7. (B) Fraction of resonant transitions as a function of the signal amplitude for a purely sinusoidal perturbation and a sinusoid plus noise (SD=2.8 pN). Data measured for R3 IVVI at the resonant frequency of 0.7 Hz.

Although the amplitude of the periodic forcing enhances the level of signal detection, stochastic resonance does not arise simply from the magnitude of the oscillating forcing applied to the system. At an amplitude of $A = 1.4$ pN, where the response at the resonance frequency is saturated, we obtain the same frequency-response dependence as that at half that amplitude, indicating that the high selectivity of talin towards the driving force is amplitude-independent (Fig. S8).

III. DISCUSSION

Our data demonstrate that talin detects force oscillations by undergoing stochastic resonance. Our most surprising result is the absence of a measurable effect of broadband mechanical noise on the folding dynamics of talin. Mechanical noise could be viewed, in a first approximation, as an increase in the effective temperature of the talin molecule along the pulling coordinate; however, we do not observe any effect of even large noise perturbations on talin folding kinetics. This is astonishing given that the noise amplitude of nearly 20 pN peak-to-peak used here dwarfs the 2 pN folding range of talin vastly. The physical basis of this noise rejection mechanism is intriguing and contrasts sharply with the exquisite sensitivity shown by talin folding to periodic signals as low as 0.6 pN peak-to-peak. Although there is clearly much about the physics of proteins folding under force that remains poorly understood, our experiments are strongly suggestive that stochastic resonance could play an essential role in the biological function of talin as a mechanosensor.

Although initially formulated in the context of nonlinear physics, stochastic resonance has been demonstrated in a broad range of biological systems, with particular emphasis as a sensory mechanism in mechanoreceptors, like the crayfish hair cells [34], the cricket cercal system [35], or the vestibular and auditory system [6, 36]. Interestingly, in all these examples, signal transduction involves the activation of gated ion channels, which convert mechanical perturbations into electrophysiological signals. However, mechanotransduction also involves biochemical signaling, where force stimuli trigger downstream signaling pathways through a complex network of interacting proteins [3–5]. In this sense, it remains yet to be explored if stochastic resonance could also play a role in mechanotransduction pathways that involve ligand binding to force-bearing proteins instead of gating of mechanosensitive channels.

Mechanical signal transduction relies on the robust and finely-tuned response of molecular force sensors. Mechanical information is both encoded in the amplitude of the signal and its time-dependent evolution. Hence, both components must be accurately deciphered and interpreted by cellular force sensors. The auditory system is the paradigm of a mechanotransduction organ [7, 37, 38]. The hair cells are responsible for sound detection and transduction into elec-

bioRxiv preprint doi: https://doi.org/10.1101/2020.01.10.901991; this version posted January 11, 2020. The copyright holder for this preprint (which was not certified by peer review) is the author/funder, who has granted bioRxiv a license to display the preprint in perpetuity. It is made available under aCC-BY-NC-ND 4.0 International license.

trical signals. Sound waves travel through the cochlea and induce vibrations on the basilar and tectorial membranes, which have a gradient of thickness and stiffness between the base and the apex. Hence, each frequency resonates at different positions along the membranes, which effectively decomposes the sound wave into its basic components that excite hair cells at different locations along the cochlea. The deflection of the hair bundles triggers the fast opening and closing of gated channels, ultimately converting the complex sound wave into nerve impulses that are interpreted by the brain. This process is highly nonlinear and has an excellent performance in the presence of noise, which indeed induces deflections of the stereocilia over a hundred times larger than those caused by threshold stimuli [29]. Hence, stochastic resonance has often been discussed to operate as an adaptive mechanism for enhanced sensitivity in the naturally noisy hearing process [6, 36, 39, 40].

In a similar sense, cells constantly receive and transmit complex force stimuli between other cells and their environment, which are converted into biochemical signals that ultimately modulate gene expression. For example, durotaxis is directed by maintained fluctuating forces that cell junctions apply to the extracellular matrix to sample its stiffness [15]. Additionally, protrusive podosomes generate oscillating forces that underpin their mechanosensing activity [41, 42]. At the protein level, single-cell measurements have demonstrated that talin experiences cyclic fluctuations with an amplitude that necessary involves folding and unfolding transitions [43]. All this recent evidence suggests the physiological relevance of force oscillations in mechanosensing; however, how cellular force sensors decompose these complex signals in a finely-tuned way remains mostly unknown.

Our results show that individual talin domains detect force oscillations in a finely-tuned way by shifting its natural stochastic dynamics to a phase-locked folding response. Importantly, the responsive frequency regime is determined by the mechanical stability of the protein domain. The 13 talin-rod domains have a graded mechanical stability and respond to the amplitude of the force signal by unfolding hierarchically upon increasing loads [24, 25]. In the context of our findings, this could suggest that each talin bundle responds to complex force signals by undergoing stochastic resonance at different frequencies correlated with their unfolding force; weak domains would respond to fast frequencies while more stable ones would detect slow oscillations. Altogether, the talin rod would resonate at different segments over its extension, providing a mechanism for signal decomposition, analogous to that in the cochlear membranes.

Ultimately, the force on talin is transduced into a biochemical signal by the recruitment of binding proteins, which is regulated by the folding status of talin domains. There are at least 11 vinculin-binding sites buried in the hydrophobic core of the 13 talin bundle domains [16, 19]. Hence, vinculin binding is force-dependent, and maximal vinculin recruitment requires sufficient load on talin to unfold all the rod domains. By contrast, other ligands such as RIAM or DLC1 bind to folded talin bundles, and are inhibited by the amplitude of the force bore by talin, often competing antagonistically with vinculin for the same substrate [16, 44]. Therefore, the transduction of force stimuli into biochemical signaling by talin is controlled by force-dependent binding constants. Our data demonstrate that the emergence of resonant dynamics shifts the distribution of folding/unfolding transitions from stochastic to deterministic dynamics, which are characterized by regularly-spaced transitions. We propose that the change from random to deterministic folding kinetics in entrained talin domains plays a vital role in the binding kinetics of its ligands. If this proves to be correct, entrained folding dynamics may provide for a mechanism to convert complex mechanical signals into Fourier-decomposed biochemical signals along the talin mechanosensor.

IV. MATERIALS AND METHODS

A. Single-Molecule Experiments

All our experiments were carried out in our custom-made magnetic tape head tweezers setup, detailed in [27]. The fluid chambers were built and functionalized, as described before [27, 45]. Protein constructs contain an N-terminal HaloTag enzyme for covalent attachment to the functionalized glass coverslip, the talin R3 domain, eight repeats of titin I91, and a C-terminal AviTag for biotinylation. Detailed expression and purification specified in SI Appendix and elsewhere [27, 45]. Experiments are carried out in PBS buffer with 10 mM ascorbic acid (pH 7.3). The data are acquired at rates between 1 to 1.6 kHz with our custom-made software, written onto a binary file, and visualized in real-time with Igor Pro 8 (Wavemetrics). Single-molecule recordings are smoothed with a Savitzki-Golay algorithm with a 101-box size (R3 IVVI) or a 31-box size (R3 WT). Recordings are idealized for analysis with a double-threshold algorithm to detect the occupations on the folded and unfolded states automatically. Further details on experimental analysis are described in SI Appendix.

bioRxiv preprint doi: https://doi.org/10.1101/2020.01.10.901991; this version posted January 11, 2020. The copyright holder for this preprint (which was not certified by peer review) is the author/funder, who has granted bioRxiv a license to display the preprint in perpetuity. It is made available under aCC-BY-NC-ND 4.0 International license.

B. Protein expression and purification

Polyprotein constructs are engineered using BamHI, BglII, and KpnI restriction sites in pFN18a restriction vector, as described previously [26]. Our protein construct contains the R3 IVVI, or R3 WT mouse talin domain, followed by eight titin I91 domains, and flanked by an N-terminal HaloTag enzyme and a C-terminal AviTag for biotinylation. Human vinculin head was expressed and purified following an analogous procedure, skipping the biotinylation process. See SI (Section XIII) for further details.

V. ACKNOWLEDGMENTS

We thank Dr. Igor Barsukov from University of Liverpool for sharing the talin plasmids with us. We thank all of the members of the J.M.F. laboratory for the valuable discussions and comments on the manuscript. This work was supported by NIH Grant GG014033.

VI. REFERENCES

[1] J. Eyckmans, T. Boudou, X. Yu, and C. S. Chen, "A hitchhiker's guide to mechanobiology," *Developmental Cell*, vol. 21, no. 1, pp. 35 – 47, 2011.

[2] P. Roca-Cusachs, V. Conte, and X. Trepat, "Quantifying forces in cell biology," *Nature Cell Biology*, vol. 19, pp. 742–751, 2017.

[3] E. C. Yusko and C. L. Asbury, "Force is a signal that cells cannot ignore," *Molecular Biology of the Cell*, vol. 25, no. 23, pp. 3717–3725, 2014. PMID: 25394814.

[4] A. W. Orr, B. P. Helmke, B. R. Blackman, and M. A. Schwartz, "Mechanisms of mechanotransduction," *Developmental Cell*, vol. 10, no. 1, pp. 11 – 20, 2006.

[5] F. Martino, A. R. Perestrelo, V. Vinarský, S. Pagliari, and G. Forte, "Cellular mechanotransduction: From tension to function," *Frontiers in Physiology*, vol. 9, p. 824, 2018.

[6] A. Hudspeth, "Making an effort to listen: Mechanical amplification in the ear," *Neuron*, vol. 59, no. 4, pp. 530 – 545, 2008.

[7] M. A. Vollrath, K. Y. Kwan, and D. P. Corey, "The micromachinery of mechanotransduction in hair cells," *Annual Review of Neuroscience*, vol. 30, no. 1, pp. 339–365, 2007.

[8] L. S. Tsimring, "Noise in biology," *Reports on progress in physics. Physical Society (Great Britain)*, vol. 77, no. 2, pp. 026601–026601, 2014.

[9] A. J. Engler, S. Sen, H. L. Sweeney, and D. E. Discher, "Matrix elasticity directs stem cell lineage specification," *Cell*, vol. 126, no. 4, pp. 677 – 689, 2006.

[10] C. E. Chan and D. J. Odde, "Traction dynamics of filopodia on compliant substrates," *Science*, vol. 322, no. 5908, pp. 1687–1691, 2008.

[11] M. J. Paszek, N. Zahir, K. R. Johnson, J. N. Lakins, G. I. Rozenberg, A. Gefen, C. A. Reinhart-King, S. S. Margulies, M. Dembo, D. Boettiger, D. A. Hammer, and V. M. Weaver, "Tensional homeostasis and the malignant phenotype," *Cancer Cell*, vol. 8, no. 3, pp. 241 – 254, 2005.

[12] L. B. Case and C. M. Waterman, "Integration of actin dynamics and cell adhesion by a three-dimensional, mechanosensitive molecular clutch," *Nature Cell Biology*, vol. 17, pp. 955 EP –, 06 2015.

[13] A. del Rio, R. Perez-Jimenez, R. Liu, P. Roca-Cusachs, J. M. Fernandez, and M. P. Sheetz, "Stretching single talin rod molecules activates vinculin binding," *Science*, vol. 323, no. 5914, pp. 638–641, 2009.

[14] R. Sunyer, V. Conte, J. Escribano, A. Elosegui-Artola, A. Labernadie, L. Valon, D. Navajas, J. M. García-Aznar, J. J. Muñoz, P. Roca-Cusachs, and X. Trepat, "Collective cell durotaxis emerges from long-range intercellular force transmission," *Science*, vol. 353, no. 6304, pp. 1157–1161, 2016.

[15] S. V. Plotnikov, A. M. Pasapera, B. Sabass, and C. M. Waterman, "Force fluctuations within focal adhesions mediate ecm-rigidity sensing to guide directed cell migration," *Cell*, vol. 151, no. 7, pp. 1513 – 1527, 2012.

[16] B. T. Goult, T. Zacharchenko, N. Bate, R. Tsang, F. Hey, A. R. Gingras, P. R. Elliott, G. C. K. Roberts, C. Ballestrem, D. R. Critchley, and I. L. Barsukov, "Riam and vinculin binding to talin are mutually exclusive and regulate adhesion assembly and turnover," *Journal of Biological Chemistry*, vol. 288, no. 12, pp. 8238–8249, 2013.

[17] K. Burridge and M. Chrzanowska-Wodnicka, "Focal adhesions, contractility, and signaling," *Annual Review of Cell and Developmental Biology*, vol. 12, no. 1, pp. 463–519, 1996.

[18] L. B. Case and C. M. Waterman, "Integration of actin dynamics and cell adhesion by a three-dimensional, mechanosensitive molecular clutch," *Nature Cell Biology*, vol. 17, pp. 955–963, 2015.

bioRxiv preprint doi: https://doi.org/10.1101/2020.01.10.901991; this version posted January 11, 2020. The copyright holder for this preprint (which was not certified by peer review) is the author/funder, who has granted bioRxiv a license to display the preprint in perpetuity. It is made available under aCC-BY-NC-ND 4.0 International license.

[19] M. D. Bass, B. Patel, I. G. Barsukov, I. J. Fillingham, R. Mason, B. J. Smith, C. R. Bagshaw, and D. R. Critchley, "Further characterization of the interaction between the cytoskeletal proteins talin and vinculin," *Biochemical Journal*, vol. 362, no. 3, pp. 761–768, 2002.

[20] M. Yao, B. T. Goult, H. Chen, P. Cong, M. P. Sheetz, and J. Yan, "Mechanical activation of vinculin binding to talin locks talin in an unfolded conformation," *Scientific Reports*, vol. 4, pp. 4610 EP –, 04 2014.

[21] R. Tapia-Rojo, A. Alonso-Caballero, and J. M. Fernandez, "Direct observation of a coil-to-helix contraction triggered by vinculin binding to talin," *bioRxiv*, 2019.

[22] J. M. Fernandez and H. Li, "Force-clamp spectroscopy monitors the folding trajectory of a single protein," *Science*, vol. 303, no. 5664, pp. 1674–1678, 2004.

[23] M. Rief, M. Gautel, F. Oesterhelt, J. M. Fernandez, and H. E. Gaub, "Reversible unfolding of individual titin immunoglobulin domains by afm," *Science*, vol. 276, no. 5315, pp. 1109–1112, 1997.

[24] A. W. M. Haining, M. von Essen, S. J. Attwood, V. P. Hytönen, and A. del Río Hernández, "All subdomains of the talin rod are mechanically vulnerable and may contribute to cellular mechanosensing," *ACS Nano*, vol. 10, pp. 6648–6658, 07 2016.

[25] M. Yao, B. T. Goult, B. Klapholz, X. Hu, C. P. Toseland, Y. Guo, P. Cong, M. P. Sheetz, and J. Yan, "The mechanical response of talin," *Nature Communications*, vol. 7, p. 11966, 2016.

[26] G. Bell, "Models for the specific adhesion of cells to cells," *Science*, vol. 200, no. 4342, pp. 618–627, 1978.

[27] R. Tapia-Rojo, E. C. Eckels, and J. M. Fernández, "Ephemeral states in protein folding under force captured with a magnetic tweezers design," *Proceedings of the National Academy of Sciences*, vol. 116, no. 16, pp. 7873–7878, 2019.

[28] L. Gammaitoni, P. Hänggi, P. Jung, and F. Marchesoni, "Stochastic resonance," *Rev. Mod. Phys.*, vol. 70, pp. 223–287, 1998.

[29] K. Wiesenfeld and F. Jaramillo, "Minireview of stochastic resonance," *Chaos: An Interdisciplinary Journal of Nonlinear Science*, vol. 8, no. 3, pp. 539–548, 1998.

[30] R. Benzi, G. Parisi, A. Sutera, and A. Vulpiani, "Stochastic resonance in climatic change," *Tellus*, vol. 34, no. 1, pp. 10–15, 1982.

[31] B. M. Jost and B. E. A. Saleh, "Signal-to-noise ratio improvement by stochastic resonance in a unidirectional photorefractive ring resonator," *Opt. Lett.*, vol. 21, pp. 287–289, Feb 1996.

[32] K. Hayashi, S. de Lorenzo, M. Manosas, J. M. Huguet, and F. Ritort, "Single-molecule stochastic resonance," *Phys. Rev. X*, vol. 2, p. 031012, Aug 2012.

[33] M. Grifoni and P. Hänggi, "Coherent and incoherent quantum stochastic resonance," *Phys. Rev. Lett.*, vol. 76, pp. 1611–1614, Mar 1996.

[34] J. K. Douglass, L. Wilkens, E. Pantazelou, and F. Moss, "Noise enhancement of information transfer in crayfish mechanoreceptors by stochastic resonance," *Nature*, vol. 365, no. 6444, pp. 337–340, 1993.

[35] J. E. Levin and J. P. Miller, "Broadband neural encoding in the cricket cereal sensory system enhanced by stochastic resonance," *Nature*, vol. 380, no. 6570, pp. 165–168, 1996.

[36] F. Jaramillo and K. Wiesenfeld, "Mechanoelectrical transduction assisted by brownian motion: a role for noise in the auditory system," *Nature Neuroscience*, vol. 1, no. 5, pp. 384–388, 1998.

[37] P. G. Gillespie and U. Müller, "Mechanotransduction by hair cells: Models, molecules, and mechanisms," *Cell*, vol. 139, pp. 33–44, 2019/11/09 2009.

[38] A. J. Hudspeth, "Integrating the active process of hair cells with cochlear function," *Nature Reviews Neuroscience*, vol. 15, pp. 600 EP –, 08 2014.

[39] Y. Roongthumskul, R. Shlomovitz, R. Bruinsma, and D. Bozovic, "Phase slips in oscillatory hair bundles," *Phys. Rev. Lett.*, vol. 110, p. 148103, 2013.

[40] B. Nadrowski, P. Martin, and F. Jülicher, "Active hair-bundle motility harnesses noise to operate near an optimum of mechanosensitivity," *Proceedings of the National Academy of Sciences*, vol. 101, no. 33, pp. 12195–12200, 2004.

[41] A. Labernadie, A. Bouissou, P. Delobelle, S. Balor, R. Voituriez, A. Proag, I. Fourquaux, C. Thibault, C. Vieu, R. Poincloux, G. M. Charrière, and I. Maridonneau-Parini, "Protrusion force microscopy reveals oscillatory force generation and mechanosensing activity of human macrophage podosomes," *Nature Communications*, vol. 5, no. 1, p. 5343, 2014.

[42] N. M. Kronenberg, P. Liehm, A. Steude, J. A. Knipper, J. G. Borger, G. Scarcelli, K. Franze, S. J. Powis, and M. C. Gather, "Long-term imaging of cellular forces with high precision by elastic resonator interference stress microscopy," *Nature Cell Biology*, vol. 19, pp. 864 EP –, 06 2017.

[43] F. Margadant, L. L. Chew, X. Hu, H. Yu, N. Bate, X. Zhang, and M. Sheetz, "Mechanotransduction in vivo by repeated talin stretch-relaxation events depends upon vinculin," *PLOS Biology*, vol. 9, pp. 1–13, 12 2011.

[44] A. W. M. Haining, R. Rahikainen, E. Cortes, D. Lachowski, A. Rice, M. von Essen, V. P. Hytönen, and A. del Río Hernández, "Mechanotransduction in talin through the interaction of the r8 domain with dlc1," *PLOS Biology*, vol. 16, pp. 1–20, 07 2018.

[45] I. Popa, J. A. Rivas-Pardo, E. C. Eckels, D. J. Echelman, C. L. Badilla, J. Valle-Orero, and J. M. Fernández, "A halotag anchored ruler for week-long studies of protein dynamics," *Journal of the American Chemical Society*, vol. 138, pp. 10546–10553, 08 2016.